Ammonium Iron(II,III) Phosphate: Hydrothermal Synthesis and Characterization of $NH_4Fe_2(PO_4)_2$

Sophie Boudin and Kwang-Hwa Lii*,†

Institute of Chemistry, Academia Sinica, Taipei, Taiwan

Received May 30, 1997

The mixed-valence iron phosphate $NH_4Fe_2(PO_4)_2$, which was synthesized by the high-temperature, high-pressure hydrothermal method, crystallizes in the monoclinic space group $C2/c$ with $a = 20.0066(1)$ Å, $b = 14.8319(2)$ Å, $c = 9.9899(1)$ Å, $\beta = 119.278(1)°$, and $Z = 16$. Its compact structure consists of chains of edge-sharing $Fe^{II}O_6$ octahedra and chains of corner-sharing $Fe^{III}O_6$ octahedra and PO_4 tetrahedra. These chains are connected to each other and delimit tunnels in the [221], [2$\bar{2}$1], and [001] directions, in which NH_4^+ cations are located. Mössbauer spectroscopy confirms the presence of Fe^{II} and Fe^{III}. The title compound is the first example of a mixed-valence ammonium iron phosphate.

Introduction

The alkali-metal iron phosphate system has yielded a wide variety of new crystalline phases under high-temperature, high-pressure hydrothermal conditions.[1] The structures of these phases consist of discrete FeO_6 octahedra, FeO_5 trigonal bipyramids, dimers of corner-sharing, edge-sharing, or face-sharing FeO_6 octahedra, trimeric, tetrameric units of Fe−O polyhedra, and infinite chains of FeO_6 octahedra sharing either trans or skew edges. They include iron(II), iron(III), and mixed-valence compounds. Using organic amines as templates, mild hydrothermal conditions lead to layered and open-framework structures.[2−6]

We are now exploring the ammonium/iron/phosphate phase space by way of high-temperature, high-pressure hydrothermal reactions. Some ammonium iron(III) phosphates have been synthesized in the past for their fertilizer's properties, but no crystal structures have been reported.[7−10] Recently the investigations in the field of the transition metal phosphates led to isolation and characterization of only four ammonium iron(III) phosphates.[11−14] One of them exists as a natural mineral, and the others were synthesized at room temperature or under mild hydrothermal conditions. In this paper we report the high-temperature, high-pressure hydrothermal synthesis, single-crystal X-ray structure, and Mössbauer spectroscopy of $NH_4Fe_2(PO_4)_2$, the first example of a mixed-valence ammonium iron phosphate.

Experimental Section

Synthesis. High-temperature, high-pressure hydrothermal synthesis was performed in gold ampules contained in a Leco Tem-Pres autoclave where pressure was provided by water pumped by a compressed air-driven intensifier. The phosphate, $NH_4Fe_2(PO_4)_2$, was initially synthesized by heating a mixture of $NH_4H_2PO_4$ (0.132 g), $(NH_4)_2HPO_4$ (0.152 g), Fe_2O_3 (0.032 g), and water (0.3 mL) in a sealed gold ampule (3.5 × 0.485 cm inside diameter) at 500 °C and an estimated pressure of 32 000 psi for 24 h, which was then cooled at 3 °C/h to 250 °C and quenched to room temperature by removing the autoclave from the furnace. The product contained black crystals of $NH_4Fe_2(PO_4)_2$ and colorless thin plates. A black prismatic single crystal was selected for structure determination. The colorless plates were not characterized because of poor crystal quality. The black color is indicative of mixed valence, and it is worthy of note that Fe_2O_3 was the only source of iron in the reaction mixture. Under these hydrothermal conditions, hydrogen could be formed by the reaction of water with the steel wall of the autoclave. Its diffusion through the gold ampule led to partial reduction of Fe^{III} to Fe^{II}. Subsequently, hydrothermal treatment of $NH_4H_2PO_4$ (0.460 g), Fe_2O_3 (0.032 g), FeO (0.0288 g), and water (0.65 mL) in a gold ampule (4.8 × 0.6 cm inside diameter) under the same reaction conditions gave a pure product of $NH_4Fe_2(PO_4)_2$, as indicated by a comparison of the X-ray powder pattern to that simulated from the atomic coordinates derived from single-crystal study. The yield was 85% based on iron.

TGA, IR, and Mössbauer Spectroscopy. Thermogravimetric analysis was performed on a Perkin-Elmer TGA 7 thermal analyzer: The sample was heated to 900 °C at 10 °C/min in air. The loss of ammonia occurs during a very large step from 100 to 650 °C. The weight loss of 5.56% is in good agreement with the theoretical one (5.64%) corresponding to the release of one NH_3 molecule and a half water molecule and the gain of a half oxygen atom per $NH_4Fe_2(PO_4)_2$ molecule. The oxidation decomposition product at 900 °C is $FePO_4$ as indicated from powder X-ray diffraction using a Siemens D5000 powder diffractometer.

† E-mail: lii@chem.sinica.edu.tw.

(1) Lii, K. H. *J. Chem. Soc., Dalton Trans*. **1996**, 819 and references therein.
(2) Cavellec, M.; Riou, D.; Greneche, J.-M.; Ferey, G. *Inorg. Chem*. **1997**, *36*, 2187 and references therein.
(3) DeBord, J. R. D.; Reiff, W. M.; Warren, C. J.; Haushalter, R. C.; Zubieta, J. *Chem. Mater*. **1997**, *9*, 1994 and references therein.
(4) Lii, K. H.; Huang, Y. F. *J. Chem. Soc., Chem. Commun*. **1997**, *14*, 1311.
(5) Lii, K. H.; Huang, Y. F. *J. Chem. Soc., Dalton Trans*. **1997**, *13*, 2221.
(6) Lii, K. H.; Huang, Y. F. *J. Chem. Soc., Chem Commun*. **1997**, *9*, 839.
(7) Frazier, A. W.; Smith, J. P.; Lehr, J. R. *J. Agric. Food Chem*. **1966**, *14*, 522.
(8) Ando, J.; Frazier, A. W.; Smith, J. P.; Lehr, J. R. *J. Agric. Food Chem*. **1968**, *16*, 691.
(9) Frazier, A. W.; et al. *J. Agric. Food Chem*. **1973**, *20*, 138.
(10) Haseman, J.; et al. *Soil. Sci. Soc. Am. Proc*. **1950**, *15*, 76.
(11) Krasnikov, V. V.; Konstant, Z. A.; Fundamenskii, V. S. *Izv. Acad. Nauk SSSR, Neorg. Mater*. **1983**, *19*, 1373.
(12) Yakubovich, O. V.; Dadashov, M. S. *Kristallografiya* **1992**, *37*, 1403.
(13) Moore, P. B.; Araki, T. *Am. Miner*. **1979**, *64*, 587.
(14) Yakubovich, O. V. *Kristallografiya* **1993**, *38*, 43.

S0020-1669(97)00655-1 CCC: $15.00
Published on Web 01/28/1998

Table 1. Crystallographic Data for $NH_4Fe_2(PO_4)_2$

chem formula	$Fe_2H_4NO_8P_2$
fw	319.68
space group	*C*2/*c*
a, Å	20.0066(1)
b, Å	14.8319(2)
c, Å	9.9899(1)
β, deg	119.278(1)
V, Å^3	2585.68(7)
Z	16
μ(Mo Kα), cm^{-1}	50.0
ρ_{calcd}, g·cm^{-3}	3.285
λ, Å	0.710 73
T, °C	23
*R*1[a]	0.0294
w*R*2[b]	0.0829

[a] $R1 = \Sigma||F_o| - |F_c||/\Sigma|F_o|$. [b] $wR2 = \{\Sigma[w(F_o^2 - F_c^2)^2]/\Sigma[w(F_o^2)^2]\}^{1/2}$; $w = 1/[\sigma^2(F_o^2) + (0.0392P)^2 + 6.00P]$, where $P = (\max(F_o^2) + 2F_c^2)/3$.

The infrared spectrum was recorded on a Perkin-Elmer Paragon 1000 FT-IR spectrometer. The presence of NH_4^+ cations in the title compound was confirmed by a large absorption band at 3047 cm^{-1} and a narrow one at 1416 cm^{-1} corresponding to the stretching and the bending vibrations of the NH_4^+ group. The ^{57}Fe Mössbauer measurements were made on a constant-acceleration instrument at room temperature. Isomer shifts are reported with respect to an iron foil standard at 300 K.

Single-Crystal X-ray Diffraction. A black prismatic crystal of dimensions 0.45 x 0.25 × 0.13 mm was selected for indexing and intensity data collection on a Siemens Smart-CCD diffractometer equipped with a normal focus, 3 kW sealed tube X-ray source. Intensity data were collected in 1200 frames with increasing ω (width of 0.3° per frame). Number of measured reflections and observed unique reflections ($F_o > 4\sigma(F_o)$): 15 104 and 2928. Agreement factor between equivalent reflections (R_{int}): 0.0505. Absorption corrections were applied with $T_{min,max} = 0.486$ and 0.889. On the basis of systematic absences, statistics of intensity distribution, and successful solution and refinement of the structure, the space group for the title compound was determined to be *C*2/*c* (No. 15). The structure was solved by direct methods: The metal and phosphorus atoms were first located, and the nitrogen, oxygen and hydrogen atoms were found in difference Fourier maps. Atomic coordinates and isotropic thermal factors of the hydrogen atoms were also refined. The final cycles of least-squares refinement including the atomic coordinates and anisotropic thermal parameters for all non-hydrogen atoms converged at $R1 = 0.0294$ and $wR2 = 0.0829$. Neutral-atom scattering factors from the *International Tables for X-ray Crystallography* (Vol. IV) for all atoms were used. Anomalous dispersion and secondary extinction corrections were applied. Structure solution and refinement were performed by using SHELXTL, Version 5.03.[15]

Results and Discussion

Structure. The crystallographic data are listed in Table 1. The atomic coordinates, interatomic distances, bond angles, and bond-valence sums are given in Tables 2 and 3, respectively. Atoms Fe(1) and Fe(2) sit on 2-fold axes, and all other atoms are at general positions. All iron atoms are octahedrally coordinated. Fe(1), Fe(2), and Fe(3) are trivalent, and Fe(4) and Fe(5) are divalent.

The compact structure of the ammonium iron phosphate $NH_4Fe_2(PO_4)_2$ is composed of edge and corner-sharing FeO_6 octahedra and PO_4 tetrahedra. A suitable description can be made by considering the projections along the [221] and [2$\bar{2}$1] directions (Figures 1 and 2). The $[Fe_2P_2O_8]_\infty$ framework contains two kinds of chains, running along the [221] and [2$\bar{2}$1] directions. The first one, noted $[FeO_4]_\infty$ and represented in dark gray, is built up from edge-sharing $Fe^{II}O_6$ octahedra in such a way that each iron polyhedron shares two skew edges with the two next polyhedra. This assemblage forms an undulating $[FeO_4]_\infty$ chain different from the rutile type chain. The second kind of chain, with the $[FePO_8]_\infty$ formulation and represented by medium and light gray polyhedra, is built up from alternating and corner-sharing $Fe^{III}O_6$ octahedra and PO_4 tetrahedra. The preference of Fe^{II} ions for the Fe(4) and Fe(5) sites can be rationalized by a smaller $Fe^{II}-Fe^{II}$ repulsion in the chain of edge-sharing FeO_6 octahedra. The two different kinds of chains are connected in such a way that each polyhedron of one $[FePO_8]_\infty$ chain shares one corner with one polyhedron of a second $[FePO_8]_\infty$ chain and one corner with one octahedron or one corner with two octahedra of one $[FeO_4]_\infty$ chain (Figure 3). More precisely, each $Fe^{III}O_6$ octahedron belonging to the $[FePO_8]_\infty$ chain shares a "free" apex of a $Fe^{II}O_6$ octahedron of the $[FeO_4]_\infty$ chain, whereas each PO_4 tetrahedron shares an apex of a common edge of the $[FeO_4]_\infty$ chain. This arrangement forms a $[Fe_6P_4O_{26}]_\infty$ tube constituted by five parallel chains; one of them presenting the [FeO4]$_\infty$ type adopts the sequence Fe(4)−Fe(5)−Fe(5)−Fe(4)..., and the four others presenting the $[FePO_8]_\infty$ type adopt the sequences P(4)−Fe(3)−P(1)−Fe(2)... and Fe(1)−P(3)−Fe(3)−P(2).... In the three-dimensional framework, the $[Fe_6P_4O_{26}]_\infty$ tubes are interconnected to each other in such a way to form a stacking of two kinds of (201) layers in which the tubes are disposed in two successive layers alternatively along the [221] and [2$\bar{2}$1] direction (Figure 1). In this arrangement, the nonparallel $[Fe_6P_4O_{26}]_\infty$ tubes are both linked

Table 2. Atomic Coordinates and Thermal Parameters (Å^2) for $NH_4Fe_2(PO_4)_2$

atom	*x*	*y*	*z*	U_{eq}[a]/U_{iso}[b]
Fe(1)	0.5	0.18089(3)	0.25	0.0101(1)
Fe(2)	0.5	0.30581(3)	0.75	0.0101(1)
Fe(3)	0.74969(2)	0.56195(2)	0.24674(4)	0.0098(1)
Fe(4)	0.57533(2)	0.43502(2)	0.09127(4)	0.0114(1)
Fe(5)	0.67213(2)	0.31055(2)	0.39793(4)	0.0116(1)
P(1)	0.64444(3)	0.46134(4)	−0.08859(7)	0.0097(1)
P(2)	0.58294(3)	0.33423(4)	0.53922(7)	0.0098(1)
P(3)	0.66647(3)	0.08687(4)	0.46451(7)	0.0098(1)
P(4)	0.60510(3)	0.20915(4)	0.08074(7)	0.0100(1)
O(1)	0.6768(1)	0.4732(1)	0.0875(2)	0.0115(3)
O(2)	0.5706(1)	0.4070(1)	−0.1318(2)	0.0129(3)
O(3)	0.6271(1)	0.5524(1)	−0.1719(2)	0.0130(3)
O(4)	0.7005(1)	0.4085(1)	−0.1211(2)	0.0136(3)
O(5)	0.6706(1)	0.3476(1)	0.6038(2)	0.0115(3)
O(6)	0.5612(1)	0.2814(1)	0.3900(2)	0.0129(3)
O(7)	0.5403(1)	0.4248(1)	0.5051(2)	0.0141(3)
O(8)	0.5667(1)	0.2804(1)	0.6504(2)	0.0139(3)
O(9)	0.7059(1)	0.1804(1)	0.4968(2)	0.0144(4)
O(10)	0.6962(1)	0.0404(1)	0.6212(2)	0.0148(4)
O(11)	0.5785(1)	0.0927(1)	0.3956(2)	0.0134(3)
O(12)	0.6859(1)	0.0341(1)	0.3563(2)	0.0140(3)
O(13)	0.6228(1)	0.3027(1)	0.1598(2)	0.0142(3)
O(14)	0.6825(1)	0.1609(1)	0.1394(2)	0.0154(4)
O(15)	0.5515(1)	0.1574(1)	0.1221(2)	0.0142(4)
O(16)	0.5701(1)	0.2163(1)	−0.0945(2)	0.0140(4)
N(1)	0.7126(2)	0.1896(2)	0.8373(3)	0.0229(5)
N(2)	0.4467(2)	−0.0646(2)	0.3400(4)	0.0337(7)
H(1)	0.666(3)	0.207(3)	0.822(5)	0.04(1)*
H(2)	0.712(2)	0.149(2)	0.765(4)	0.026(9)*
H(3)	0.726(2)	0.171(3)	0.919(5)	0.03(1)*
H(4)	0.740(3)	0.225(3)	0.837(5)	0.04(1)*
H(5)	0.444(3)	−0.079(4)	0.433(7)	0.07(2)*
H(6)	0.482(4)	−0.032(4)	0.367(7)	0.09(2)*
H(7)	0.443(4)	−0.106(5)	0.269(8)	0.11(2)*
H(8)	0.398(3)	−0.041(3)	0.299(6)	0.07(2)*

[a] U_{eq} is defined as one-third of the trace of the orthogonalized $\mathbf{U}_{ij}$ tensor. [b] U_{iso} is indicated by an asterisk.

(15) Sheldrick, G. M. *SHELXTL PC*, Version 5; Siemens Analytical X-Ray Instruments, Inc.: Madison, WI, 1995.

Table 3. Selected Bond Lengths (Å), Bond Angles (deg), and Bond-Valence Sums (Σs) for $NH_4Fe_2(PO_4)_2$

Fe(1)−O(6)	2.000(2)					
Fe(1)−O(6)	2.000(2)	83.7(1)				
Fe(1)−O(11)	2.015(2)	169.42(7)	89.13(7)			
Fe(1)−O(11)	2.015(2)	89.13(7)	169.42(7)	99.0(1)		
Fe(1)−O(15)	2.026(2)	90.73(7)	104.07(7)	83.49(7)	83.70(7)	
Fe(1)−O(15)	2.026(2)	104.07(7)	90.73(7)	83.70(7)	83.49(7)	160.2(1)
Σs(Fe(1)−O) = 3.02		O(6)	O(6)	O(11)	O(11)	O(15)
Fe(2)−O(2)	2.002(2)					
Fe(2)−O(2)	2.002(2)	82.9(1)				
Fe(2)−O(8)	2.053(2)	106.85(7)	89.17(7)			
Fe(2)−O(8)	2.053(2)	89.17(7)	106.85(7)	158.8(1)		
Fe(2)−O(16)	2.003(2)	168.10(7)	90.86(7)	83.11(7)	82.89(7)	
Fe(2)−O(16)	2.003(2)	90.86(7)	168.10(7)	82.89(7)	83.11(7)	96.9(1)
Σs(Fe(2)−O) = 2.98		O(2)	O(2)	O(8)	O(8)	O(16)
Fe(3)−O(1)	2.030(2)					
Fe(3)−O(4)	2.043(2)	104.89(7)				
Fe(3)−O(5)	2.033(2)	82.16(7)	81.81(7)			
Fe(3)−O(10)	1.954(2)	88.51(7)	90.75(7)	166.13(8)		
Fe(3)−O(12)	2.046(2)	82.09(7)	171.53(7)	104.17(7)	84.56(7)	
Fe(3)−O(14)	1.944(2)	167.52(8)	83.06(7)	89.62(7)	101.15(8)	90.91(7)
Σs(Fe(3)−O) = 3.08		O(1)	O(4)	O(5)	O(10)	O(12)
Fe(4)−O(1)	2.126(2)					
Fe(4)−O(2)	2.223(2)	66.74(6)				
Fe(4)−O(3)	2.076(2)	92.73(7)	155.83(7)			
Fe(4)−O(7)	2.031(2)	152.66(7)	91.77(7)	111.37(7)		
Fe(4)−O(7)	2.229(2)	82.34(7)	86.33(7)	104.12(7)	79.47(7)	
Fe(4)−O(13)	2.142(2)	88.38(7)	86.77(7)	79.74(7)	107.89(7)	170.07(7)
Σs(Fe(4)−O) = 2.20		O(1)	O(2)	O(3)	O(7)	O(7)
Fe(5)−O(3)	2.194(2)					
Fe(5)−O(5)	2.143(2)	82.61(7)				
Fe(5)−O(6)	2.225(2)	85.50(7)	66.54(6)			
Fe(5)−O(9)	2.123(2)	167.99(7)	86.41(7)	85.68(7)		
Fe(5)−O(9)	2.137(2)	106.89(7)	93.43(7)	155.34(7)	78.54(7)	
Fe(5)−O(13)	2.086(2)	78.32(7)	152.63(7)	92.37(7)	110.18(7)	110.75(7)
Σs(Fe(5)−O) = 2.09		O(3)	O(5)	O(6)	O(9)	O(9)
P(1)−O(1)	1.559(2)					
P(1)−O(2)	1.548(2)	100.7(1)				
P(1)−O(3)	1.534(2)	111.8(1)	112.1(1)			
P(1)−O(4)	1.527(2)	110.8(1)	111.9(1)	109.3(1)		
Σs(P(1)−O) = 4.90		O(1)	O(2)	O(3)		
P(2)−O(5)	1.558(2)					
P(2)−O(6)	1.546(2)	101.11(9)				
P(2)−O(7)	1.537(2)	111.8(1)	111.4(1)			
P(2)−O(8)	1.526(2)	111.3(1)	112.1(1)	109.1(1)		
Σs(P(2)−O) = 4.91		O(5)	O(6)	O(7)		
P(3)−O(9)	1.549(2)					
P(3)−O(10)	1.539(2)	106.6(1)				
P(3)−O(11)	1.548(2)	113.3(1)	105.5(1)			
P(3)−O(12)	1.531(2)	109.0(1)	112.6(1)	109.9(1)		
Σs(P(3)−O) = 4.90		O(9)	O(10)	O(11)		
P(4)−O(13)	1.550(2)					
P(4)−O(14)	1.538(2)	106.6(1)				
P(4)−O(15)	1.531(2)	109.1(1)	111.8(1)			
P(4)−O(16)	1.538(2)	112.4(1)	106.2(1)	110.6(1)		
Σs(P(4)−O) = 4.94		O(13)	O(14)	O(15)		
N(1)−H(1)	0.91(5)		N(2)−H(5)	0.98(6)		
N(1)−H(2)	0.93(4)		N(2)−H(6)	0.79(7)		
N(1)−H(3)	0.78(4)		N(2)−H(7)	0.92(7)		
N(1)−H(4)	0.76(5)		N(2)−H(8)	0.92(6)		

and interpenetrated to each other; linked by a common edge between P(1) or P(2) tetrahedra of one layer and Fe(4) or Fe(5) octahedra, respectively, of a successive layer and interpenetrated insofar as each $Fe^{III}O_6$ octahedron belongs to two $[FePO_8]_\infty$ chains of two successive (201) layers. The $[Fe_2P_2O_8]_\infty$ framework delimits tunnels along the [221] and [2$\bar{2}$1] directions (Figure 1 and 2) and along *c* (Figure 4), in which the NH_4^+ cations are located. Each of the two crystallographically independent N(1) and N(2) atoms is surrounded by four nearest hydrogen atoms with distances ranging from 0.76(5) to 0.98(6) Å and by ten and nine oxygen atoms, respectively, with N--O distances ranging from 2.817(3) to 3.341(3) Å. The closest distances between the O atoms and the H atoms are equal to 1.98(7), 1.99(7), and 2.08(7) Å.

It is worth pointing out that this structure obtained by high-pressure synthesis is characterized by a large density (3.285 g/cm3) involving numerous short Fe−P, P−N, and N−N distances about equal to 2.8 (×2), 3.6 (×7), and 3.35 Å

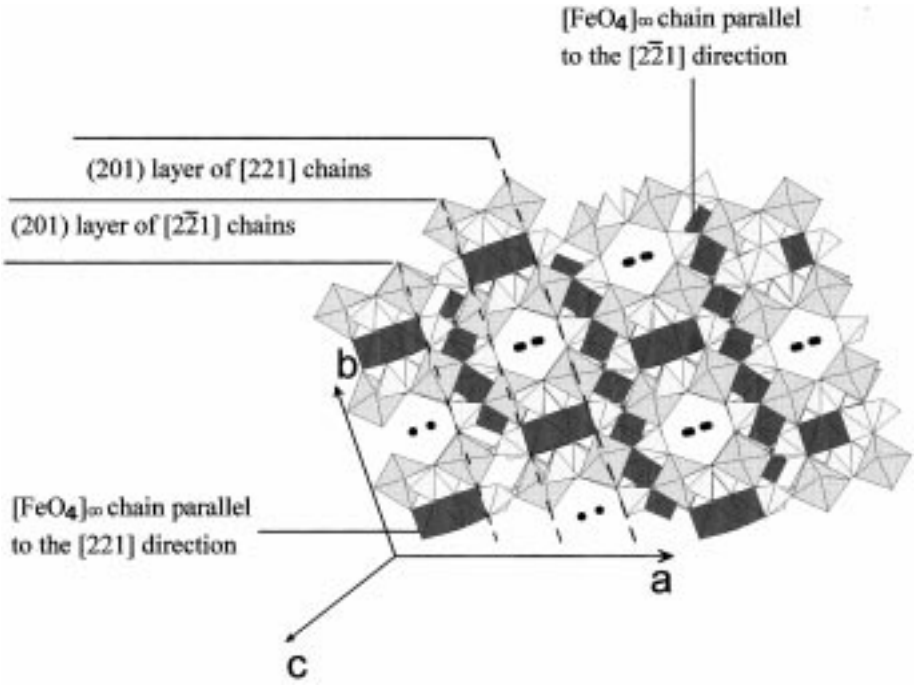

Figure 1. Polyhedral representation of the $NH_4Fe_2(PO_4)_2$ structure projected along the [221] direction. $Fe^{II}O_6$ octahedra are represented in a dark gray pattern, $Fe^{II}IO_6$ octahedra in a medium gray pattern, and PO_4 tetrahedra in a light gray pattern. H atoms are omitted for clarity.

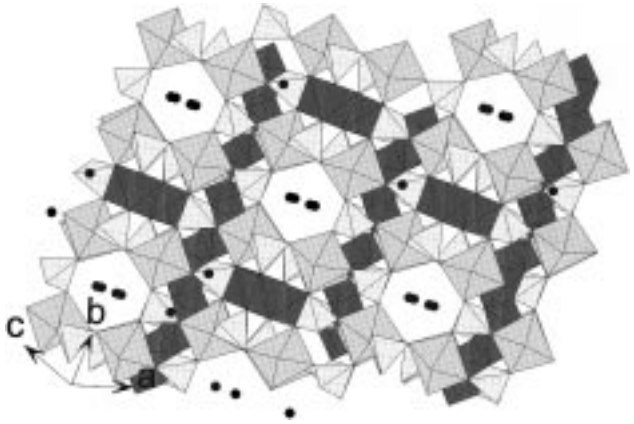

Figure 2. Polyhedral representation of the $NH_4Fe_2(PO_4)_2$ structure projected along the [2$\bar{2}$1] direction.

Table 4. Mössbauer Parameters of $NH_4Fe_2(PO_4)_2$ at 300 K

site	isomer shift/Fe^0 (mm/s)	quadrupole splitting (mm/s)	full width at half-height (mm/s)	intensity (%)
1	0.44	0.50	0.36, 0.34	50
2	1.20	3.14	0.40, 0.40	50

(×3), respectively. In order to check the existence of short N−N distances, the full occupancies of the nitrogen atoms have been confirmed by failed refinements with half-occupancies for the N sites, giving higher *R* factors and negative thermal factors for the nitrogen atoms. N−N distances equivalent to those observed in $NH_4Fe_2(PO_4)_2$ are rare but have been reported in two other phosphates: NH_4VOPO_4[16] and $(NH_4)_8(P_8O_{24})Te(OH)_6(H_2O)_2$[17] with the values 3.343 and 3.433 Å, respectively.

The ammonium iron phosphates observed up to now in the literature, $NH_4FeHP_3O_{10}$,[11] $NH_4Fe_2(OH)(PO_4)_2(H_2O)_2$,[12] $NH_4Fe_3[PO_3(OH)_{0.666}O_{0.333}]_3(PO_2(OH)_2)_3 \cdot 6H_2O$,[13] and $NH_4Fe(HPO_4)_2$,[14] synthesized under mild hydrothermal conditions, present lower densities equal to 2.46, 2.69, 2.36, and 2.66 g/cm^3, respectively. Their structures present also lower dimensionalities of the distribution of the iron species. Three of them are

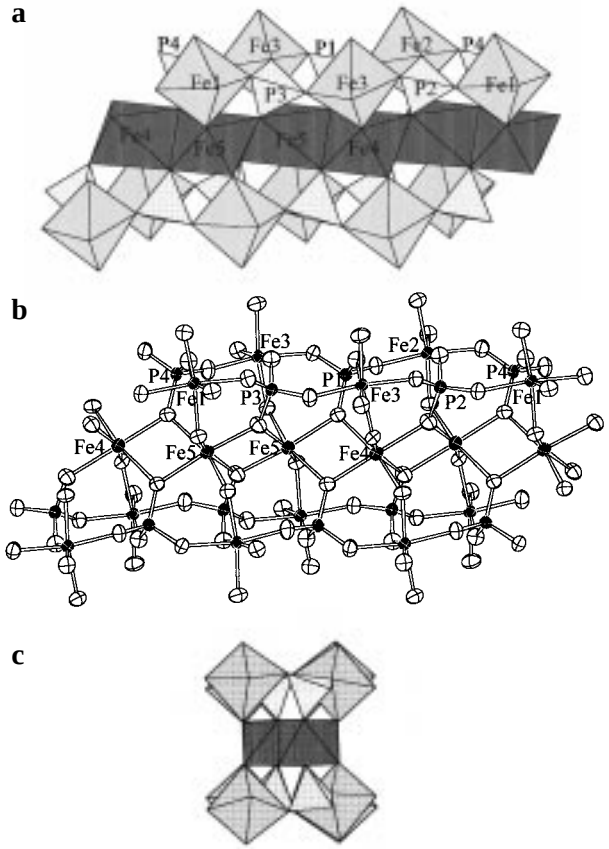

Figure 3. View of one $[Fe_6P_4O_{26}]_\infty$ tube constituted by one $[FeO_4]_\infty$ chain and four $[FePO_8]_\infty$ chains. (a) Projection perpendicular to the [2$\bar{2}$1] direction with a polyhedral representation. (b) Projection perpendicular to the [2$\bar{2}$1] direction with the 90% probability displacement ellipsoids. Fe and P atoms are represented with black ellipsoids, O atoms with white ellipsoids. (c) Projection along the [221] direction with a polyhedral representation.

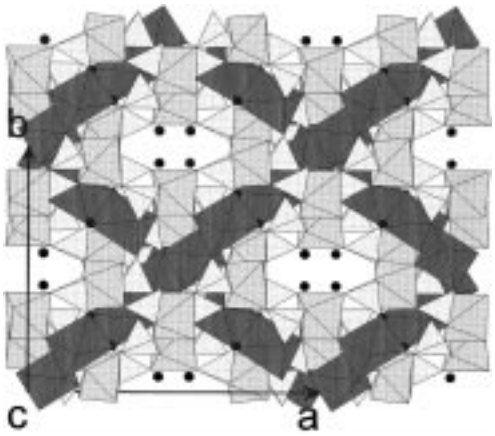

Figure 4. Polyhedral representation of the $NH_4Fe_2(PO_4)_2$ structure projected along *c*.

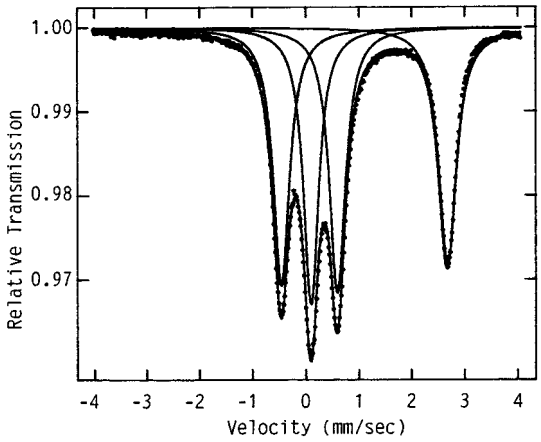

Figure 5. Mössbauer spectrum of $NH_4Fe_2(PO_4)_2$ at room temperature.

actually composed of isolated FeO_6 octahedra,[11,13,14] and the fourth one is composed of tetrameric units of octahedra.[12]

Mössbauer Spectroscopy. The ^{57}Fe Mössbauer spectrum recorded at room temperature (Figure 5) can be fitted with only two paramagnetic Mössbauer sites instead of five as expected from the crystallographic study (Table 4). The first component with an isomer shift characteristic of Fe^{III} can be assigned to Fe(1), Fe(2), and Fe(3). The second one with an isomer shift typical of Fe^{II} can be assigned to Fe(4) and Fe(5). The isomer shifts in area ratio 1:1 obtained for the two Mössbauer sites confirm the presence and the equivalent proportions of Fe^{II} and Fe^{III} species in $NH_4Fe_2(PO_4)_2$. The second component has a very large quadrupole splitting, which is similar to that observed in the Fe^{II} phosphate $SrFe_3(P_2O_7)_2$.[18]

In conclusion $NH_4Fe_2(PO_4)_2$ is the first example of an ammonium iron phosphate obtained hydrothermally under high temperature and high pressure. This synthetic method performed with NH_4^+ cations in solution allows on one hand to isolate compact structures containing ammonium and on the other hand to obtain reduced and/or mixed-valence transition metal phosphates. Further research to synthesize novel ammonium transition metal phosphates is in progress.

Acknowledgment. We thank the Institute of Chemistry, Academia Sinica, and the National Science Council (Grant NSC86−2113-M-001−014) for support, Ms. F.-L. Liao and Professor S.-L. Wang at National Tsing Hua University for X-ray intensity data collection, and Professor T.-Y. Dong at National Sun Yat-Sen University for Mössbauer spectroscopy measurements.

Supporting Information Available: Tables giving crystal data and details of the structure determination and anisotropic thermal parameters (3 pages). Ordering information is given on any current masthead page.

IC970655+

(16) Haushalter, R. C.; Chen Qu.; Soghomoniam, V.; Zubieta, J.; O'Connor, C. *J. Solid State Chem.* **1994**, *108*, 128.
(17) Averbuch-Pouchot, M. T.; Durif, A. *Acta Crystallogr.* **1993**, *C49*, 361.
(18) Lii, K. H.; Shih, P. F.; Chen, T. M. *Inorg. Chem.* **1993**, *32*, 4373.